

# SUN-AVOIDANCE SLEW PLANNING ALGORITHM WITH POINTING AND ACTUATOR CONSTRAINTS

Mohammad Ayoubi\* and Junette Hsin†

This paper presents a geometric approach for a sun (or any bright object) avoidance slew maneuver with pointing and actuator constraints. We assume spacecraft has a single light-sensitive payload with control-torque and reaction wheels' angular momentum constraints. Furthermore, we assume the initial and final attitudes, instrument boresight vector, and sun vector are known. Then we use Pontryagin's minimum principle (PMP) and derive the desired or target-frame quaternions, angular velocity and acceleration. In the end, a Monte Carlo simulation is performed to show the viability of the proposed algorithm with control-torque and angular momentum constraints.

## NUMERICAL SIMULATION

The proposed algorithm was examined by running cases in which the initial, final, and sun position vectors were randomized. Consider a spacecraft as a rigid body with one sensitive instrument. The orientation of the boresight of the instrument to the spacecraft body axes, the current and final (desired) positions with respect to the inertial frame, and the location of the sun vector are known. Only one exclusion zone around a bright object (the sun) is considered. The initial and final positions are outside of the exclusion zone.

### SAS Algorithm Pseudocode

1. Find: sequence of slew maneuvers to avoid sun vector
  - (a) Check the sun vector intrusion
    - i. Find eigenaxis  $\hat{e} = \frac{\hat{P}_i \times \hat{P}_f}{|\hat{P}_i \times \hat{P}_f|}$
    - ii. Compute  $\alpha = \frac{\pi}{2} - \cos^{-1}(\hat{S} \cdot \mathcal{N} \hat{e})$
    - iii. IF  $|\alpha| < \epsilon_p$ , THEN find  $\vec{S}_{||} = \hat{S} \cos \alpha$
  - (b) Compute  $\phi_1$ :  $\phi_1 = \cos^{-1}(\hat{P}_i \cdot \mathcal{G} \hat{S}_{||}) - \epsilon_p$
  - (c) Compute  $\phi_2$ :
    - i. IF  $\alpha \neq 0$ , THEN  $\phi_2 = 2 \sin^{-1} \left( \frac{\sin \epsilon_p}{\sin \theta} \right)$ ,  $\theta = \cos^{-1}(\hat{P}_1 \cdot \hat{S})$

\* Associate Professor, Department of Mechanical Engineering, Santa Clara University, 500 El Camino Real, Santa Clara, CA 95053 U.S.A. AIAA senior member, AAS senior member.

† Engineer, Dynamics and Control Analysis Group, Maxar Space Solutions (formerly Space Systems/Loral), 3825 Fabian Way, Palo Alto, CA 94303 U.S.A.

- ii. IF  $\alpha = 0$ , THEN  $\phi_2 = \pi$
- (d) Compute  $\phi_3$ :  $\phi_3 = \cos^{-1}(\hat{G}\hat{P}_f \cdot \hat{P}_2)$

2. Find: commanded angular velocity, angular acceleration, and quaternion profiles

- (a) Compute  $\phi_t = \frac{\dot{\phi}_{max}^2}{\ddot{\phi}_{max}}$
- (b) Compute  $t_1, t_2$ , and  $t_f$ .  
 IF  $\phi > \phi_t$ , THEN :  

$$t_1 = t_0 + \frac{\dot{\phi}_{max} - \dot{\phi}_0}{\ddot{\phi}_{max}}$$

$$t_2 = t_1 + \frac{1}{\ddot{\phi}_{max}} \left[ \phi_f - \dot{\phi}_0(t_1 - t_0) - \frac{1}{2}\ddot{\phi}_{max}(t_1 - t_0)^2 - \frac{\dot{\phi}_{max}(\dot{\phi}_{max} - \dot{\phi}_f)}{\ddot{\phi}_{max}} + \frac{(\dot{\phi}_{max} - \dot{\phi}_f)^2}{2\ddot{\phi}_{max}} \right]$$

$$t_f = t_1 + \frac{1}{\ddot{\phi}_{max}} \left[ \phi_f - \dot{\phi}_0(t_1 - t_0) - \frac{1}{2}\ddot{\phi}_{max}(t_1 - t_0)^2 + \frac{(\dot{\phi}_{max} - \dot{\phi}_f)^2}{2\ddot{\phi}_{max}} \right].$$
 ELSE:  

$$t_f = \sqrt{\frac{\dot{\phi}_{max}^2}{\ddot{\phi}_{max}}}$$

$$t_2 = t_f/2$$

$$t_1 = t_2$$
- (c) Find  ${}^D R^N$ :  ${}^D R^N = [(\cos\phi)I_{3 \times 3} + (1 - \cos\phi)\hat{e}\hat{e}^T - (\sin\alpha)E^x]$
- (d) Find  ${}_{\mathcal{B}}\dot{\omega}^D$ :  ${}_{\mathcal{B}}\dot{\omega}^D = {}^D R^N \ddot{\phi}_{max} \cdot {}_{\mathcal{N}}\hat{e}$
- (e) Solve for control torque,  $u$ :  $J \cdot {}_{\mathcal{B}}\dot{\omega}^D = u - {}_{\mathcal{B}}\omega^C \times J \cdot {}_{\mathcal{B}}\omega^C$
- (f) FOR each  $\phi$  between switching times, propagate  $\omega$  and  $q$  between switching times by solving above eqn and  $\dot{q} = \frac{1}{2}\Omega q$   
 where

$$\Omega = \begin{bmatrix} 0 & \omega_3 & -\omega_2 & \omega_1 \\ -\omega_3 & 0 & -\omega_1 & \omega_2 \\ \omega_2 & -\omega_1 & 0 & \omega_3 \\ -\omega_1 & \omega_2 & -\omega_3 & 0 \end{bmatrix}$$

with correct  $u$  for each switching time interval.

The results show that the angular velocity and acceleration never exceed the velocity and acceleration constraints for any axis. There is no noise modeled in the actuator system, as the purpose of this simulation was to validate the slewing maneuvers described by the algorithm.

The attitude and rates were computed within each switching time interval for a constant control torque. For example, in the case of  $\phi_2$  for the interval from  $t_0$  to  $t_1$ , the torque in the inertial frame was found from  $\tau = J\ddot{\phi}_{max}$ , where  $J$  is the inertia of the SC in the body frame, and  $\ddot{\phi}_{max}$  is the desired (maximum) acceleration in the body frame. However,  $\ddot{\phi}_{max}$  needs to go the sun vector  ${}_{\mathcal{N}}S$ , which is fixed in the inertial frame. To find  $\ddot{\phi}_{max}$ , the rotation from the inertial to (desired) body frame needed to be calculated, which is possible from  ${}^D R^N = [(\cos\phi)I_{3 \times 3} + (1 - \cos\phi)\hat{e}\hat{e}^T - (\sin\alpha)E^x]$ .

With the desired direction of acceleration known, the necessary control torque can be solved for from Euler's equations for rigid body dynamics  $J \cdot {}_{\mathcal{B}}\dot{\omega}^D = u - {}_{\mathcal{B}}\omega^C \times J \cdot {}_{\mathcal{B}}\omega^C$ . Though real

spacecraft have multiple bodies and flexible appendages, the spacecraft was assumed to be a rigid body for algorithm demonstration purposes. Once  $u$  is solved, the propagation of  $\omega$  and  $q$  was performed by discretely solving the dynamical and kinematic equations of motion with a simulation rate of 100 Hz. The process was repeated for the interval from  $t_1$  to  $t_2$ , except the torque applied was 0. For  $t_2$  to  $t_f$ , the acceleration applied was  $-\ddot{\phi}_{max}$ , as the spacecraft needed to slew down to reach its final point for that leg of the slew.

Two cases are shown here - one in which the sun angle is greater than 0 from the slew plane. The other case is one in which the sun vector lies directly on the slew plane, so that  $\phi_2 = 180$  degrees.

### Case I: $\alpha > 0$

The parameters for a test case in which the sun vector did not lie directly on the slew plane are shown in Table 1. The calculated slew angles are shown in Table 2.

The constraints for maximum angular velocity and acceleration were chosen to demonstrate that the angular velocity and acceleration profiles would follow the switching times if-else statements, should the  $\phi$  exceed the angle threshold  $\phi_t$ . The spacecraft slews from the initial to the target position during the maneuvers, and  $P_1$  and  $P_2$  are connected via a rotation around the sun vector. This is found to be true no matter the sun vector's position relative to the slew plane.

**Table 1. Initial, Final, and Sun Positions in Inertial Frame and Constraints (Sample Inputs)**

Unit Vector	Comp
$P_i$	[-0.50, 0.57, 0.65]
$P_f$	[0.76, -0.48, -0.44]
$S$	[0.30, -0.50, -0.81]
Parameter	Constraint
$\alpha_{max}$	1 $rad/s^2$
$\omega_{max}$	1 $rad/s$

**Table 2. Slew Angles  $\phi_1$ ,  $\phi_2$ , and  $\phi_3$**

$\phi$	deg
1	32.08
2	102.56
3	17.76

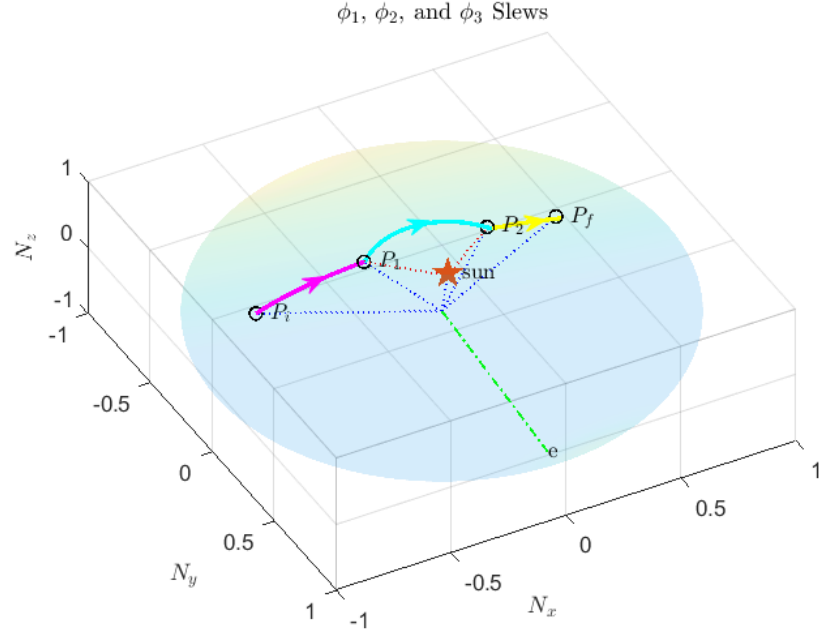


**Figure 1. Attitude Profile of the Entire Slew.**

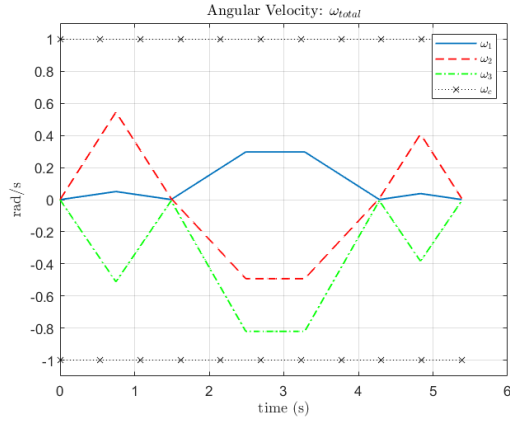


**Figure 2. Angular Velocity when  $\alpha > 0$ .**

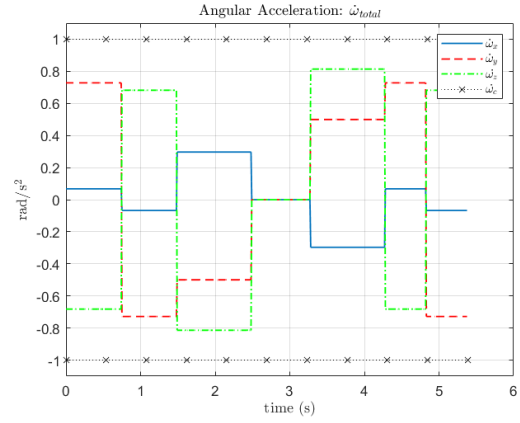


**Figure 3. Angular Acceleration when  $\alpha > 0$ .**

Only the angular velocity and acceleration plots have constraints. In real life, the spacecraft's reaction wheels' ability to impart angular momentum is translated to a constraint in angular velocity, and the thrusters ability to impose torque translates to a constraint in angular acceleration. Therefore, there is no torque constraint plotted.

Due to the high velocity and acceleration constraints, there is no coasting period for the  $\phi_1$  and  $\phi_3$  portions of the slew. However, there is a period of 0 angular acceleration constant angular velocity

for  $\phi_2$ , which is reflected in the Figures 2 and 3. The attitude and torque profiles are shown in Figures 4 and 5.

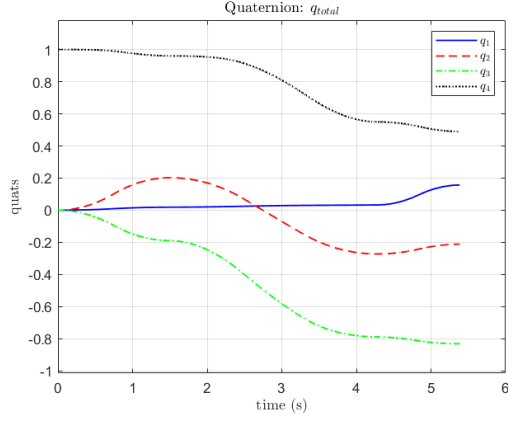


**Figure 4. Quaternions when  $\alpha > 0$ .**

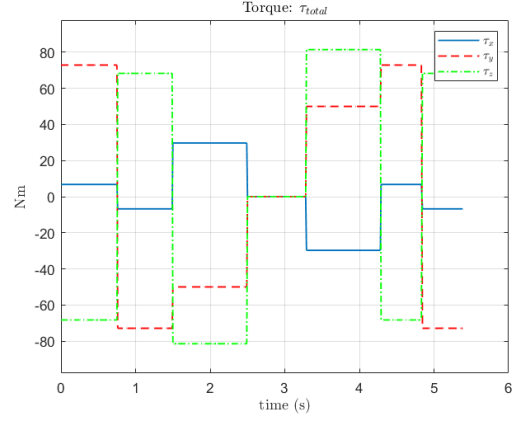


**Figure 5. Torque when  $\alpha > 0$ .**

### Case II: $\alpha = 0$

For the case in which the sun vector lies directly on the slew plane,  $\phi_2 = 180$  degrees. The initial, final, and sun positions in the inertial frame and the constraints are in Table 3.

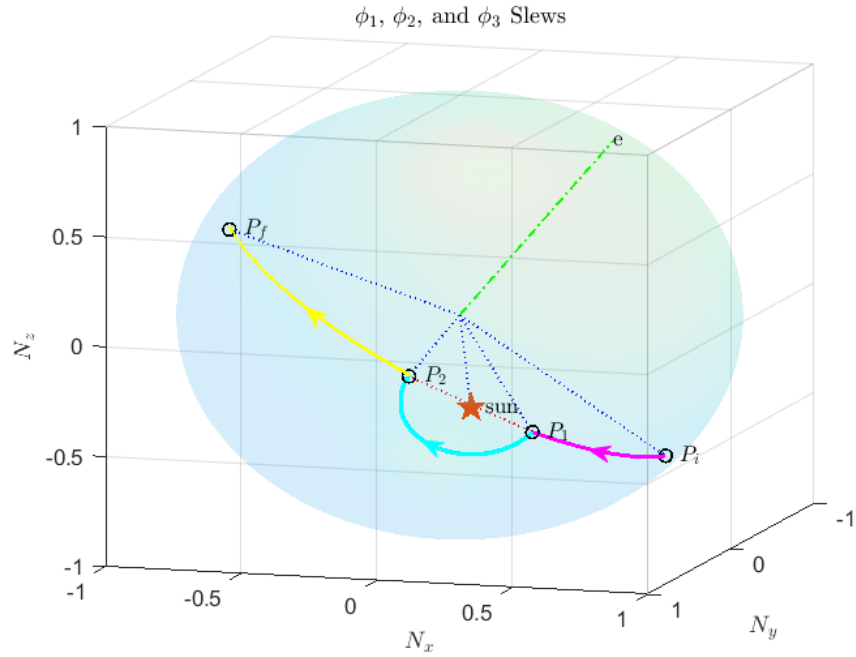


**Figure 6. Attitude Profile of the Entire Slew when  $\alpha = 0$ .**

The previous case, in which  $\alpha > 0$ , had acceleration and velocity constraints of  $1 \text{ rad/s}^2$  and  $1 \text{ rad/s}$  respectively, to demonstrate the if-else statements for switching times in case  $\phi > \phi_t$ . For this example, much more realistic constraints were imposed to reflect how the acceleration and velocity profiles would look like in real life.

**Table 3. Initial, Final, and Sun Positions in Inertial Frame and Constraints (inputs)**

Unit Vector	Comp
$P_i$	[0.65, -0.35, -0.67]
$P_f$	[-0.93, -0.25, 0.28]
$S$	[-0.20, -0.78, -0.59]
Parameter	Constraint
$\alpha_{max}$	$0.02 \text{ rad/s}^2$
$\omega_{max}$	$0.01 \text{ rad/s}$

**Table 4. Slew Angles  $\phi_1, \phi_2$ , and  $\phi_3$**

$\phi$	deg
1	41.82
2	180.00
3	62.45

With smaller constraints, the simulation takes much longer to complete the slew maneuvers. Figures 7 and 10 show that the torque and acceleration applied are very short compared to the duration of the entire maneuver, in contrast to Figures 3 and 5. The spacecraft spends the majority of the time coasting at constant angular velocity, as seen in Figure 8. Though the initial and final points are further apart in the gyrostat unit sphere to begin with, the simulation takes an order of magnitude longer to complete at almost 500 seconds for  $\alpha = 0$ , as opposed to almost 5.5 seconds for  $\alpha > 0$ . The case shown here is much more realistic example that reflects real-world conditions.

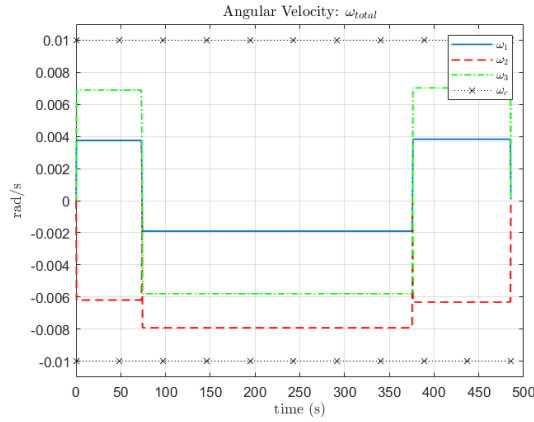


**Figure 7. Angular Velocity when  $\alpha = 0$ .**

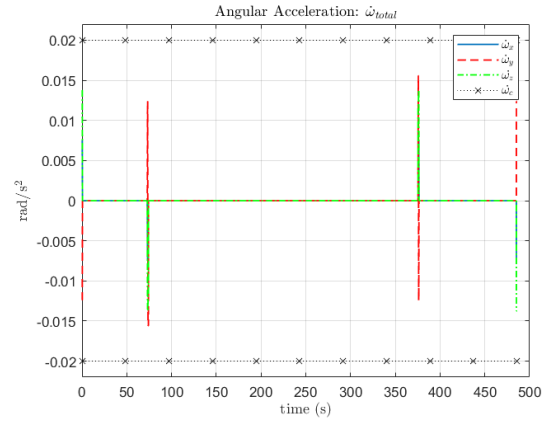


**Figure 8. Angular Acceleration when  $\alpha = 0$ .**

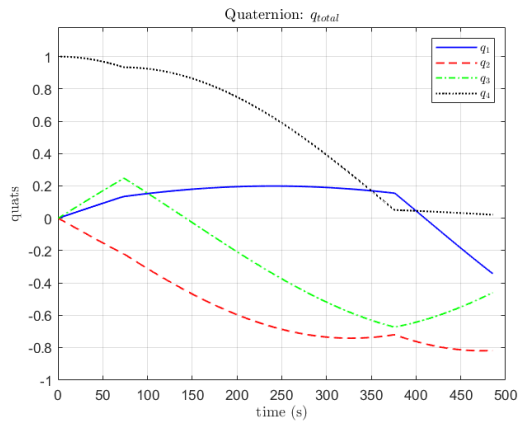


**Figure 9. Quaternions when  $\alpha = 0$ .**

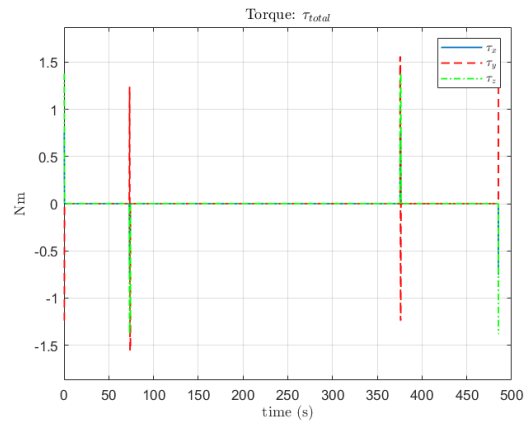


**Figure 10. Applied Torque when  $\alpha = 0$ .**